Effective electron-density dependence of the magnetocrystalline anisotropy in highly chemically ordered pseudobinary $(Fe_{1-x}Mn_x)_{50}Pt_{50}$ $L1_0$ alloys

Gereon Meyer[1] and Jan-Ulrich Thiele[2]
[1]*Stanford Synchrotron Radiation Laboratory, 2575 Sand Hill Road, Menlo Park, California 94025, USA*
[2]*San Jose Research Center, Hitachi Global Storage Technologies, 650 Harry Road, San Jose, California 95120, USA*
(Received 1 February 2006; revised manuscript received 13 April 2006; published 23 June 2006)

The magnetic and structural properties of highly chemically ordered epitaxial $(Fe_{1-x}Mn_x)_{50}Pt_{50}$ $(0 \leqslant x \leqslant 0.68)$ thin films were investigated. This study complements earlier experimental studies on pseudobinary ternary and quaternary FePt-based alloys, providing a more complete picture of the dependence of the magnetization and magnetocrystalline anisotropy on structural properties and effective electron density in the chemically ordered $3d$ transition metal–Pt $L1_0$ alloy system. Maximum anisotropy and magnetization are found for the undoped FePt composition, and increasing Mn additions result in a steady reduction of magnetocrystalline anisotropy and saturation magnetization. Comparing the results of our experimental study to two recent computational first-principles studies of pseudobinary $L1_0$ alloys, we find a significantly more rapid reduction of magnetization and anisotropy with decreasing effective electron density than predicted by either of the two theories. This reduction may be explained in part by the antiparallel alignment of Fe and Mn moments observed in circular x-ray magnetic dichroism.

DOI: 10.1103/PhysRevB.73.214438 PACS number(s): 75.30.Gw, 75.50.Bb

I. INTRODUCTION

Among the thin-film and superlattice systems exhibiting high magnetocrystalline anisotropy, the $L1_0$ phases of the binary alloy FePt and the related pseudobinary $3d$-$5d$ transition metal alloys of the type $(XY)_{50}Pt_{50}$ $(X,Y = Cr,Mn,Fe,Co,Ni)$ have in recent years attracted great interest as a model system for fundamental studies of the microscopic origin of magnetic phenomena as well as for potential technological applications. The $L1_0$ phase of the binary alloys, often referred to as the face-centered-tetragonal (fct) or CuAu(I) phase, consists of a monatomic, chemically modulated natural superlattice of the two elements. In the pseudobinary alloys the superlattice consists of Pt layers alternating with layers of randomly distributed $3d$ transition metals. The unit cell of the $L1_0$ phase is a tetragonally distorted face-centered-cubic cell with the c axis defined to lie perpendicular to the planes of the chemical superlattice. The extent of this distortion, i.e., the ratio of the c axis to the a axis (c/a ratio) is one of the important parameters describing the structure and influencing many of the magnetic properties of the $L1_0$ phase.[1] In most cases for a given composition the c/a ratio is inversely proportional to the degree of long-range chemical order; for completely disordered materials, i.e., materials with the $3d$ transition metal(s) and the Pt randomly distributed on the lattice sites, a face-centered-cubic unit cell with a c/a ratio of 1 is observed, and with increasing chemical order the c/a ratio decreases. Specifically, for the series of alloys with a filled s band for fully chemically ordered materials the c/a ratio varies as a function of the $3d$ element as listed in Table I, following the successive filling of the d bands from $n_{\mathrm{eff}}=7$ $(3d^5s^2)$ for MnPt to $n_{\mathrm{eff}}=10$ $(3d^8s^2)$ for NiPt (note, only the $3d$ electrons are taken into account in this notation of the effective number of valence electrons, n_{eff}; the contribution of the $5d$ electrons of Pt is assumed to be constant and therefore not included). The case of the antiferromagnetic $L1_0$ phase of CrPt,[2,3] $n_{\mathrm{eff}}=6$, deviates from the systematic changes observed in the other alloys due to the incompletely filled s orbital of Cr $(3d^5s^1)$.

The $L1_0$ phases of FePt and CoPt are ferromagnetic,[4–6] and for highly chemically ordered films grown with the direction of the c axis normal to the film plane these structures exhibit very large perpendicular magnetic anisotropy.[7] These attributes make these alloys attractive base materials for future ultrahigh-density magnetic recording applications such as thermally or heat-assisted magnetic recording.[8] NiPt is also ferromagnetic at low temperatures, but paramagnetic at room temperature, with a Curie temperature of about 150 K.[9] In contrast, MnPt is a well-known antiferromagnet[10–12] that is widely used in thin-film technological applications, e.g., as a pinning layer in magnetoresistive sensors.[13,14] In recent years the fundamental understanding of the correlation of the structural properties, the electronic structure and magnetic properties such as the magnetocrystalline anisotropy K_U and the Curie temperature T_C has started to emerge.[1,15,16] This has been accompanied by steady progress in the experimental capabilities to grow high-quality epitaxial and polycrystalline films with a wide range of desired properties such as longitudinal[17,18] or perpendicular[19,20] orientation of the easy axis of magnetization and high energy product or coercivity (see, e.g., Refs. 21 and 22).

For a given FePt or CoPt composition the magnetization, apart from a small contribution due to the polarization of the Pt, is almost independent of the degree of chemical order. In contrast, the magnetocrystalline anisotropy is proportional to the degree of chemical order and for FePt ranges from below 1×10^5 erg/cm^3 for films with order parameter $S=0$ to 7×10^7 erg/cm^3 for films with $S\sim1$.[23] In band structure calculations using a linear muffin-tin orbital approach for fully chemically ordered FePt and CoPt Sakuma found a direct dependence of the magnetocrystalline anisotropy on the c/a ratio, showing maximum anisotropy for the case of FePt and a c/a ratio close to the experimental value of 0.96.[1] However, in a recent computational study using full-potential linear muffin-tin orbital and exact muffin-tin orbital ap-

 ©2006 The American Physical Society

TABLE I. Valence electron configuration, effective electron density n_{eff}, c/a ratio, and room-temperature magnetic phase of the four $3d^n s^2$-Pt alloys and CrPt.

Alloy	Configuration	n_{eff}	c/a ratio	Magnetic phase at $T=300$ K	Reference
CrPt	$3d^5s^1$	6	0.99	Antiferromagnetic	2 and 3
MnPt	$3d^5s^2$	7	0.918	Antiferromagnetic	10–12
FePt	$3d^6s^2$	8	0.957	Ferromagnetic	4 and 5
CoPt	$3d^7s^2$	9	0.98	Ferromagnetic	6
NiPt	$3d^8s^2$	10	0.93	Paramagnetic	9

proaches, Burkert *et al.* reported that for the case of constant c/a ratio and varying effective electron density n_{eff}, Mn substitutions in FePt result in a further steady increase of the magnetic anisotropy energy of up to 33% compared to FePt for Mn concentrations up to $x=0.25$ ($n_{\mathrm{eff}}=7.75$).[24] Such an increase in anisotropy could potentially be very significant for technological applications such as high-anisotropy media for magnetic recording and permanent magnet applications.[8] Experimentally the c/a ratio and n_{eff} cannot be easily adjusted independently while maintaining full chemical order. However, the c/a ratio and n_{eff} can be varied simultaneously by substituting for Fe other $3d$ elements with a different total number of $3s$ and $3d$ valence electrons n_{eff}, where $n_{\mathrm{eff}}=6,7,8,9,10$ for Cr, Mn, Fe, Co, Ni, respectively. In experimental studies on a number of pseudobinary $(XY)_{50}\mathrm{Pt}_{50}$ alloys by Suzuki *et al.*[25] ($X,Y=\mathrm{Cr,Fe,Ni,Co}$) and Thiele *et al.*[26] ($X=\mathrm{Fe},Y=\mathrm{Ni}$), it was found that indeed pseudobinary alloys with almost complete chemical order can be grown and that the lattice constants and c/a ratio change steadily between the values of the respective binary alloys. In both studies maximum anisotropy and magnetization was found for $n_{\mathrm{eff}}\sim 8$, i.e., the FePt composition, confirming the results of the band structure calculations in Ref. 1. However, few experimental data have been published on the pseudobinary alloy $(\mathrm{FeMn})_{50}\mathrm{Pt}_{50}$. In one earlier experimental study of the structural and magnetic properties of $(\mathrm{Fe}_{1-x}\mathrm{Mn}_x)\mathrm{Pt}$ powder samples using neutron and x-ray diffraction a rich magnetic phase diagram with several collinear and noncollinear ferromagnetic and antiferromagnetic phases was found for samples with reasonably high chemical order.[27] The results of this study, in particular the dependence of the saturation magnetization M_S on n_{eff}, show the same general trend as the results on $(\mathrm{Fe}_{1-x}\mathrm{Cr}_x)\mathrm{Pt}$ thin films, namely, a steady drop of M_S with increasing Mn content,[25] even though $M_S=0$ is reached for slightly different values of n_{eff}, at $n_{\mathrm{eff}}=7$ for $(\mathrm{Fe}_{1-x}\mathrm{Cr}_x)\mathrm{Pt}$ and $n_{\mathrm{eff}}=7.75$ for $(\mathrm{Fe}_{1-x}\mathrm{Mn}_x)\mathrm{Pt}$. This finding contradicts the computational study of Burkert *et al.* where a slight increase in magnetization and a strong increase in anisotropy are predicted for increasing Mn content in the range $0\leqslant x\leqslant 0.25$.[24] Here we present an experimental study on structural and magnetic properties of epitaxial $(\mathrm{Fe}_{1-x}\mathrm{Mn}_x)\mathrm{Pt}$ thin films with very high degrees of chemical order, and high crystalline quality, complementing the experimental data of Refs. 25 and 27 and allowing a direct comparison with the theoretical predictions of Refs. 1 and 24.

II. EXPERIMENT

FeMnPt (001) samples were deposited epitaxially on MgO (100) substrates by magnetron cosputtering from two alloy targets $\mathrm{Fe}_{55}\mathrm{Pt}_{45}$ and $\mathrm{Mn}_{41}\mathrm{Pt}_{59}$, in a commercial sputter system (AJA International). An Ar gas pressure of 3 mTorr was used for sputtering, and the deposition rate was approximately 0.5 Å/s. The substrate temperature was set at 550 °C during deposition, and in order to minimize effects of interdiffusion on sample composition only very thin seed layers of about 10 Å Fe followed by 10 Å Pt were used. For the chosen alloy compositions of the targets and deposition parameters the resulting Pt content is 50 ± 3 at. %, and the Fe and Mn concentrations of the $(\mathrm{Fe}_{1-x}\mathrm{Mn}_x)\mathrm{Pt}$ films were varied in the range $0\leqslant x\leqslant 0.68$. Film thicknesses and compositions were measured by particle-induced x-ray emission (PIXE) and Rutherford Backscattering (RBS). The composition along with the structural and magnetic parameters of all samples used in this study are listed in Table II.

The epitaxial quality, degree of chemical ordering, and lattice constants for the epitaxial films were determined from specular and grazing incidence (1° beam incidence angle) x-ray diffraction using a PANalytical X'pert system with Cu $K\alpha$ radiation ($\lambda=1.541$ Å). The lattice parameter perpendicular to the film plane, c, was determined from the (001), (002), and (003) peaks, and the in-plane lattice parameter a was determined from the (200) peak. The long-range order parameter was calculated from the ratios of the absorption-corrected, integrated intensities multiplied by the square of the full width at half maximum of the rocking scan of the (001) and (003) superlattice peaks to the (002) fundamental peak, following the procedures described, e.g., in Refs. 28, 23, and 29. The values reported below were taken as the averages of the two values obtained from the two superlattice peaks. It is worth noting that the theoretical maximum order parameter varies as a function of $3d$ transition metal, i.e., the sum of Fe and Mn, to Pt ratio and is given by $S_{\mathrm{max}}=1-2\Delta x$, where Δx is the deviation from equiatomic composition. For the composition range of $47<$ Pt content <53 at. % S_{max} varies from 0.94 to 1.

Hysteresis loops as well as saturation magnetization M_S and anisotropy constant K_1 were measured in a maximum field of 2 T using a commercial vibrating sample magnetometer (VSM, model DMS 10, ADE Technologies). The first-order anisotropy constant K_1 of the uniaxial magnetocrystalline anisotropy K_U is defined as $K_1=K_1^{\mathrm{eff}}+2\pi M_S^2$. K_1^{eff} was measured using a 45° method and high-field extrapolation.[30]

X-ray absorption spectra of the Fe and Mn $L_{2,3}$ edges were taken through measurement of the total electron yield at normal incidence using the vector magnet setup at beamline 4 of the Advanced Light Source (ALS).[31] A magnetic field of 0.5 T was applied alternately parallel and antiparallel to the

TABLE II. Composition, effective electron density, out-of-plane (c) and in-plane (a) lattice parameters, c/a ratio, theoretical maximum S_{max}, and experimentally determined value S_{expt}, of the long-range chemical order parameter, saturation magnetization M_S, and uniaxial anisotropy K_1 of the series of $(Fe_{1-x}Mn_x)Pt$ films discussed here.

Composition	n_{eff}	c (Å)	a (Å)	c/a	S_{max}	S_{expt}	M_S (emu/cm^3)	K_1 (10^7 erg/cm^3)
$Fe_{53}Pt_{47}$	8	3.705	3.858	0.960	0.94	0.93	1130	4.4
$(Fe_{0.99}Mn_{0.01})_{53}Pt_{47}$	7.99	3.706	3.854	0.962	0.94	0.90	1110	4.4
$(Fe_{0.98}Mn_{0.02})_{52}Pt_{48}$	7.99	3.702	3.866	0.957	0.96	0.90	1050	4.1
$(Fe_{0.97}Mn_{0.03})_{52}Pt_{48}$	7.97	3.702			0.96	0.86	1000	2.9
$(Fe_{0.95}Mn_{0.05})_{52}Pt_{48}$	7.95	3.701			0.96	0.91	1000	2.6
$(Fe_{0.92}Mn_{0.08})_{51}Pt_{49}$	7.93	3.700	3.879	0.954	0.98	0.85	930	2.2
$(Fe_{0.89}Mn_{0.11})_{50}Pt_{50}$	7.89	3.698			1	0.87	835	1.7
$(Fe_{0.81}Mn_{0.19})_{50}Pt_{50}$	7.81	3.693	3.904	0.946	1	0.88	690	1.2
$(Fe_{0.71}Mn_{0.29})_{49}Pt_{51}$	7.70	3.680	3.920	0.938	0.98	0.85	390	0.4
$(Fe_{0.57}Mn_{0.43})_{48}Pt_{52}$	7.57	3.674	3.946	0.931	0.96	0.85	133	0
$(Fe_{0.32}Mn_{0.68})_{47}Pt_{53}$	7.32	3.634	3.964	0.917	0.94	0.87	0	0

photon helicity to determine the x-ray magnetic circular dichroism (XMCD). To check for surface segregation and oxidation effects in addition core level x-ray photoemission spectra were taken in a commercial spectrometer (Phi Quantum 2000 ESCA) using monochromatic Al K_α ($h\nu = 1486.6$ eV) radiation at perpendicular and grazing emission.

III. RESULTS & DISCUSSION

A. X-ray diffraction

At equiatomic composition FePt in its chemically disordered phase forms a face-centered-cubic unit cell with Fe and Pt randomly distributed on the lattice sites. As mentioned above, the chemically ordered $L1_0$ phase of FePt comprises a natural superlattice of alternating Fe and Pt atomic planes along the (001) direction, which here coincides with the growth direction. The magnetic properties of FePt are strongly correlated with the structural properties of the material, i.e., the crystallographic orientation of the film, the degree of chemical order, and the degree of epitaxy, which is quantified by the mosaic spread. These can be determined from specular (θ-2θ geometry) x-ray diffraction (XRD) measurements. Figure 1(a) shows the XRD scans of $Fe_{52}Pt_{48}$, $(Fe_{0.92}Mn_{0.08})_{51}Pt_{49}$, and $(Fe_{0.57}Mn_{0.43})_{48}Pt_{52}$ films. A slight line broadening is observed with increasing Mn content, and the mosaic spread in the (002) reflection peaks increases from 0.5° for the FePt film, comparable to that of high-quality molecular-beam-epitaxy- (MBE-) grown FePt films reported in the literature,[32] to about 0.7° for $x=0.43$. The intense (001) and (003) superstructure peaks observed in all samples are characteristic of the chemically ordered $L1_0$ phase. From the integrated intensities of the (001), (002), and (003) peaks the degree of long-range chemical ordering, S, along the c axis can be quantified.[7] A high degree of chemical order with order parameters $S>0.85$, close to the theoretical maximum for the compositions used here, was observed in all films. In the scan of the FeMnPt films in Fig. 1(a) an additional small peak at $2\theta=47.2°$ is observed. This peak can be assigned to the (111) orientation of the $L1_0$ phase and is indicative of an inclusion of a small amount of material with a different crystallographic orientation. From the integrated intensity of the peak it can be estimated that the volume fraction of these inclusions makes up less than 1% of the film. Similar or smaller amounts of inclusions were found in all films included in the data analysis. Together the high degree of chemical order and the almost complete absence of additional diffraction peaks in specular as well as in grazing incidence scans shows that indeed the FeMnPt is growing in the same face-centered-tetragonal unit cell as FePt with Mn substituting for Fe in the pseudobinary alloy. This is further supported by the change in the lattice parameters as a function of Mn content x, plotted in Fig. 1(b). For comparison, the lattice parameters of bulk samples (open symbols) of $Fe_{50}Pt_{50}$ (Ref. 28) and $Mn_{50}Pt_{50}$ (Ref. 12) and the powder sample data by Menshikov *et al.*[27] (dotted line) are shown. Within the experimental errors good agreement between all three data sets is found, showing with increasing Mn content a steady decrease of the lattice constant perpendicular to the film c and a slightly steeper increase of the in-plane lattice constant a approaching the bulk values of MnPt at around $x=0.6$.[27] Accordingly, the c/a ratio that describes the degree of distortion of the face-centered-tetragonal unit cell decreases from 0.96 for the $Fe_{53}Pt_{47}$ film to 0.92 for the $(Fe_{0.32}Mn_{0.68})_{47}Pt_{53}$ film, again in reasonably good agreement with the data of Ref. 27.

B. Magnetic properties

Figures 2(a)–2(c) show the hysteresis loops of FePt, $(Fe_{0.92}Mn_{0.08})_{51}Pt_{49}$, and $(Fe_{0.71}Mn_{0.29})_{49}Pt_{51}$ films, respectively. All three films exhibit the easy axis of magnetization perpendicular to the plane. For the two films with $x=0$ and 0.08 the sharp drop of magnetization at the nucleation field H_N and the low remanence are indicative of low resistance to

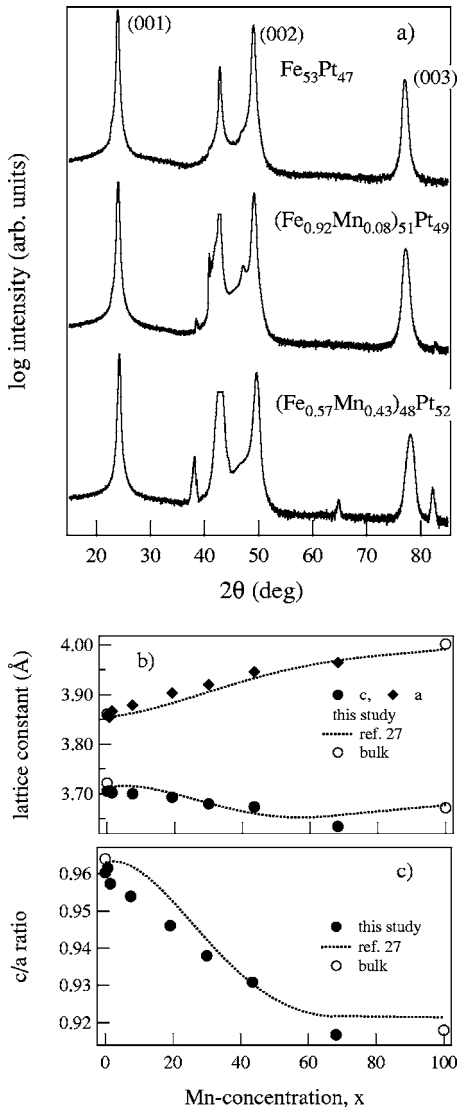

FIG. 1. (a) θ-2θ x-ray diffraction scans of 750-Å-thick $Fe_{53}Pt_{47}$, $(Fe_{0.92}Mn_{0.08})_{51}Pt_{49}$, and $(Fe_{0.57}Mn_{0.43})_{48}Pt_{52}$ (001) films grown on single-crystalline MgO (100) substrates. (b) Lattice constants perpendicular to the plane, c, and in the plane, a, of the films as a function of Mn content for part of the series of 750-Å-thick $(Fe_{1-x}Mn_x)Pt$ films listed in Table II, and (c) the c/a ratio for the same series of films.

the movement of domain walls and, by implication, low density of pinning sites in the films.[33] For the film with $x=0.29$ the hysteresis loops measured perpendicular to and in the plane of the film show only a weak perpendicular orientation. Figure 3 shows M_S and K_1 at room temperature as a function of the Mn concentration. M_S drops steadily from 1125 ± 60 emu/cm^3 for the $Fe_{53}Pt_{47}$ film, reaching $M_S=0$ approximately at $(Fe_{0.5}Mn_{0.5})Pt$, indicating a paramagnetic or antiferromagnetic state. Similarly, the anisotropy constant K_1 drops rapidly from about 4.4×10^7 erg/cm^3 for $Fe_{53}Pt_{47}$ to 1.7×10^7 erg/cm^3 for $(Fe_{0.92}Mn_{0.08})_{51}Pt_{49}$, and reaches 0 at a slightly lower Mn content, for the $(Fe_{0.57}Mn_{0.43})_{48}Pt_{52}$ sample. Note that the value of $K_1=4.4\times10^7$ erg/cm^3 for the $Fe_{53}Pt_{47}$ film is consistent with that found in other films deposited under similar conditions,[29] but somewhat lower than

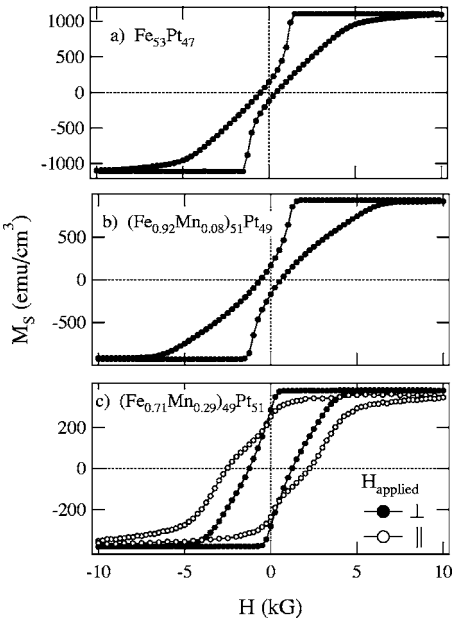

FIG. 2. Magnetic hysteresis loops measured in a vibrating sample magnetometer of 750-Å-thick $Fe_{53}Pt_{47}$, $(Fe_{0.92}Mn_{0.08})_{51}Pt_{49}$, and $(Fe_{0.71}Mn_{0.29})_{49}Pt_{51}$ films grown on single-crystalline MgO (100) substrates. The solid symbols correspond to a field applied perpendicular to the film, open symbols correspond to a field applied in the plane of the film.

that of MBE-grown films, where up to 7×10^7 erg/cm^3 has been observed.[32]

To investigate the relative magnetic orientation of the Fe and Mn moments XMCD measurements on a few selected samples were performed. Surprisingly, for samples across the whole composition range we see a sign change between the dichroism observed at the Fe and Mn edges, indicating a net antiferromagnetic alignment of the two moments, as shown for a $(Fe_{0.92}Mn_{0.08})_{51}Pt_{49}$ film in Fig. 4. From the relative areas of the absorption peaks it can be estimated that within the experimental errors the composition within the information depth of the XMCD measurements[34] of about 25 Å is identical to that of the bulk of the film as measured by RBS. Furthermore, we can exclude oxidation effects, since multiplet peaks indicating MnO in the $L_{3,2}$ XMCD spectra[35] are absent in our data. Based on these observations we can exclude the possiblilty that the opposite sign of the XMCD effect for Mn and Fe is an artifact due to, e.g., segregation of

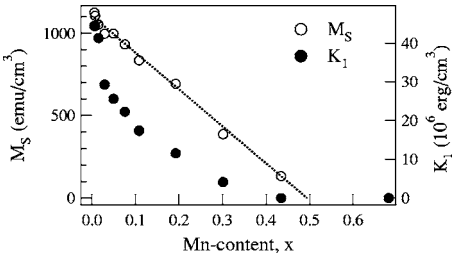

FIG. 3. Saturation magnetization and magnetocrystalline anisotropy of the series of $(Fe_{1-x}Mn_x)Pt$ films listed in Table II as a function of the Mn content.

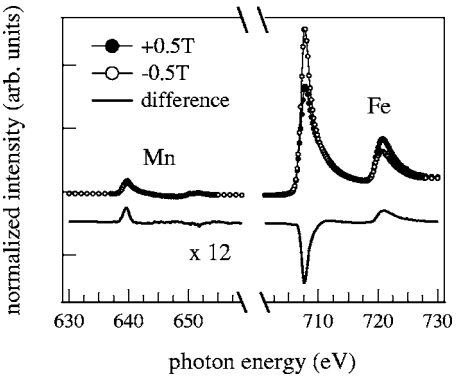

FIG. 4. X-ray absorption spectra for opposite magnetic fields (top curves) and difference spectra indicating the magnetic circular dichroism (bottom curves) of a $(Fe_{0.92}Mn_{0.08})_{51}Pt_{49}$ film. The difference spectrum of Mn was multiplied by a factor of 12.

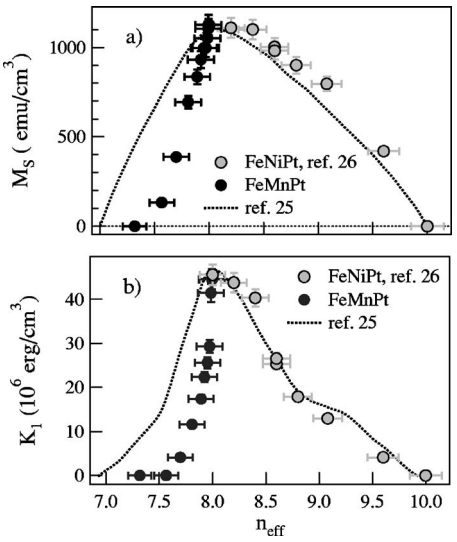

FIG. 5. (a) Saturation magnetization and (b) magnetocrystalline anisotropy of the same series of $(Fe_{1-x}Mn_x)Pt$ films shown in Fig. 3 and listed in Table II (closed symbols) and a series of $(Fe_{1-x}Ni_x)_{55}Pt_{45}$ films from Ref. 26 (open symbols) as a function of the effective electron density. The dotted lines are the dependencies predicted by the theory developed in Ref. 1 and adapted to pseudobinary alloys in Ref. 25.

one species toward the surface and the formation of Mn or MnO clusters coupled antiferromagnetically to the ferromagnetic film underneath. However, a comparison of the XMCD intensities at the $L_{3,2}$ edges of Fe and Mn shows the Mn signal to be far lower than the Fe signal. Using simple sum rule considerations,[36] assuming the ratio of numbers of $3d$ holes of Mn and Fe to be 5:4, and neglecting orbital contributions, we roughly estimate the net Mn moment per atom to be only about 25–30 % of the Fe moment. According to the neutron diffraction data measured by Menshikov *et al.* on chemically ordered powder samples, the magnetic moment per (Fe, Mn) atom should be higher for MnPt ($4.3\mu_B$) than for FePt ($3.0\mu_B$), and for ternary $(Fe_{1-x}Mn_x)_{50}Pt_{50}$ alloys a ferromagnetic phase with intermediate moments was observed for $0 \leqslant x \leqslant 25$ at. %.[27] In contrast, XMCD measurements of submonolayer Mn on Fe(100) showed antiferromagnetic coupling between Mn and Fe even for very low coverage, and a steep drop of the net Mn moment with increasing coverage, approaching zero, i.e., complete antiferromagnetic coupling within the Mn layer, for a complete monolayer.[37] Similarly a net antiferromagnetic alignment of the Fe and Mn moments was observed here, but it is worth pointing out that indeed this is a net effect, and local ferromagnetic coupling between a minority of the Fe and Mn atoms cannot be excluded based solely on such XMCD data.

IV. DISCUSSION

In the following the results of the present study are discussed in the context of the earlier experimental studies and specifically compared to the conflicting theoretical predictions by Sakuma[1] and Burkert *et al.*[24] As described above, we do not observe in our experimental study the increase in magnetization and magnetocrystalline anisotropy predicted by Burkert *et al.* for Mn content up to $x=0.25$, but qualitatively our data do follow the theoretical prediction of Ref. 1. Quantitatively, however, they also exhibit some significant differences from both the predictions based on this theory and the experimental data for $(Fe_{1-x}Cr_x)Pt$.[25] Figure 5 shows the saturation magnetization and the magnetocrystalline anisotropy, plotted here as a function of the effective electron density. Also shown are experimental data from Ref. 26 for a series of $(Fe_{1-x}Ni_x)_{55}Pt_{45}$ films and the theoretical curves taken from Ref. 25. The effective electron density was calculated using a linear interpolation between the values for MnPt, $n_{eff}=7$, FePt, $n_{eff}=8$, and NiPt, $n_{eff}=10$. Not shown in this figure are the experimental data from Ref. 27. However, we note that in the data presented here the vanishing of the ferromagnetic moment occurs at a higher Mn content, about $x=0.5$, compared to the earlier neutron diffraction data, where antiferromagnetic order at room temperature was observed for Mn content of only about $x=0.25$. Comparing the data for the films of the present study to the experimental data for $(Fe_{1-x}Cr_x)Pt$ and the theoretical curve in Ref. 25, evidently, the drop in both magnetization and anisotropy is significantly steeper in the case of $(Fe_{1-x}Mn_x)Pt$. To understand this difference it is helpful to look first at the differences between the MnPt and CrPt alloys. While both these alloys form a chemically ordered, antiferromagnetic $L1_0$ phase,[14,38] the simple d-band-filling argument made in Ref. 25 for the series from Mn $3d^5s^2$ to Ni, $3d^8s^2$ does not apply to Cr due to its different electronic configuration, $3d^5s^1$, with a half-filled s orbital but the same number of d electrons as Mn. This difference is apparent in the trend of the c/a ratio for these alloys given in Table I, with $c/a \sim 1$ for CrPt, but significant tetragonal distortion for the other alloys, and MnPt actually exhibiting the smallest value of the series with $c/a=0.92$. While no detailed structural data are reported in Ref. 25, given the large difference in c/a ratio between CrPt and MnPt and the general observation that the c/a ratio of the ternary alloys tends to assume intermediate values between those of the respective binary alloys, it seems plausible to assume that the c/a ratio will change in qualitatively different ways with effective electron density for the ternary

alloys $(Fe_{1-x}Cr_x)Pt$ and $(Fe_{1-x}Mn_x)Pt$. Given the importance of the tetragonal distortion of the fcc unit cell for the magnetocrystalline anisotropy of the $L1_0$ materials found in theoretical studies,[1,12] it further seems plausible to expect different magnetic properties of these ternary systems at equivalent effective electron densities. It is interesting to note in this context that in Sakuma's original study[1] the c/a ratio was varied but n_{eff} was kept constant at the values for FePt and CoPt.

According to Mryasov *et al.* the magnetic properties of the chemically ordered $L1_0$ phase of alloys of Fe with a nominally nonmagnetic 5*d* element like Pt are determined by a "direct" Fe-Fe interaction term between an Fe atom and its four nearest neighbors in the Fe layer, and an "indirect" Fe-Pt-Fe interaction mediated by the polarization of the Pt in the adjacent layers.[39] The hybridization of the Fe 3*d* bands with the Pt 5*d* bands and the resulting magnetic polarization of Pt has been experimentally observed for submonolayer coverage of Pt on Fe using spin-polarized photoemission[40] and in Fe-Pt multilayers using XMCD, where an induced moment of about $0.5\mu_B$ has been estimated.[41] The magnetic phase diagram of the $L1_0$ structure of MnPt observed by neutron diffraction is more complicated. As a function of temperature and composition transitions between configurations with the magnetic moment of the Mn parallel or in the plane perpendicular to the *c* axis of the $L1_0$ structure were observed, but within the experimental errors no indication of an induced moment in the Pt was found.[13] Some of the features of this magnetic phase diagram have been reproduced by linear muffin-tin orbital band structure calculations by Umetsu *et al.*[42] In this study also a large value of the magnetocrystalline anisotropy of about 1.4×10^7 erg/cm^3 was reported for the antiferromagnetic $L1_0$ phase, of the same order as that of FePt and consistent with experimental studies of exchange bias in bilayer systems. However, while this value was derived assuming only exchange splitting and spin-orbit coupling but no induced moment in the Pt as the origin of the magnetocrystalline anisotropy, the exact value of the induced moment in Pt still seems to be the subject of debate.[42,43]

For pseudobinary 3*d* TM-Pt $L1_0$ alloys the 3*d* transition metals are randomly distributed within the layer, so the net direct and indirect interaction terms for a given site will depend on the species of the four nearest neighbors within this layer. Following Ref. 27 one would assume that the exchange between two Cr atoms, $J_{\mathrm{Cr\text{-}Cr}}$, or two Mn atoms, $J_{\mathrm{Mn\text{-}Mn}}$, on neighboring sites in the same layer of the chemically ordered structure is always negative, i.e., antiferromagnetic, while that between two Fe atoms, $J_{\mathrm{Fe\text{-}Fe}}$, is always positive, i.e., ferromagnetic. The properties of a ternary alloy then depend critically on the value and sign of the exchange between the two 3*d* elements, here $J_{\mathrm{Fe\text{-}Mn}}$, and the probability and distribution of possible combinations of nearest-neighbor configurations for a given composition. The observation of a net antiparallel orientation of the Fe and Mn moments in the XMCD spectra seems to suggest that the exchange term $J_{\mathrm{Fe\text{-}Mn}}$ is antiferromagnetic over the whole concentration range. For example, assuming the values for the Mn and Fe moments given in Ref. 27 for the $(Fe_{0.92}Mn_{0.08})Pt$ film of Fig. 4 a purely collinear configuration would require almost 40% of the Mn moments to be aligned parallel to the Fe moments. The remaining 60% of the Mn moments would then be aligned antiparallel to the Fe moment, resulting in an apparent reduction of the Mn net moment as observed in XMCD.[37] It can be speculated that the partial antiparallel alignment of the Mn moments is one of the reasons for the experimentally observed reduction of the saturation magnetization and the magnetocrystalline anisotropy compared to the predictions of Ref. 24. According to the model outlined in Refs. 39 and 44 one of the main contributions to the anisotropy in FePt is the polarization of the Pt by the interactions with the neighboring Fe layers—to first order these are proportional to the effective moment of these layers. Partial antiparallel alignment within the FeMn layer in the case of the pseudobinary alloy would then not only result in a direct reduction of the saturation magnetization, but also lead to a reduction in the polarization of the Pt layer and consequently the magnetocrystalline anisotropy mediated by this polarization. It should be noted that this line of argument is strictly valid only for a collinear configuration, and that in the geometry used here XMCD is only sensitive to the perpendicular component of the magnetization. However, in their neutron diffraction study Menshikov *et al.* found a more complicated magnetic phase diagram with a canted ferromagnetic (so-called FAF) phase in the range $0.2\leqslant x\leqslant 0.26$ at room temperature, and a canted antiferromagnetic (AF) phase for $0.26<x\leqslant 0.5$. The FAF phase consists of magnetic moments with a ferromagnetic component along the *c* axis and antiferromagnetic order in the plane perpendicular to the *c* axis.[27] To reconcile the results of Ref. 27 with the XMCD data presented here as a next step a more detailed investigation using XMCD measurements at variable incidence angle probing both in-plane and out-of-plane components of the magnetic moment combined with band structure calculations to establish an estimate for $J_{\mathrm{Fe\text{-}Mn}}$ will be required.

As for the qualitative discrepancy between the magnetic properties of the $(Fe_{1-x}Mn_x)Pt$ films presented here as well as the $(Fe_{1-x}Mn_x)Pt$ powder samples presented in Ref. 27 and the theoretical predictions for this pseudobinary alloy in Ref. 24, we note that for the theoretical study the structural parameters compiled by Villars,[45] $c=3.788$ Å, $a=3.861$ Å, and $c/a=0.981$ for FePt were used across the whole composition range. These values deviate significantly from the values typically found in experimental studies on both thin film and bulk samples. For FePt we find values of $c=3.71$ Å, $a=3.86$ Å, and $c/a=0.96$, very similar to the values found in high-quality samples grown by sputter deposition under similar conditions,[29] in high-quality MBE-grown samples,[32] and in bulk samples.[27] For the $L1_0$ phase of MnPt this discrepancy between the structural parameters used in Ref. 24, $c/a=0.981$, and the experimental value $c/a=0.92$,[12] becomes even larger. As demonstrated in Ref. 1 this could lead to significant changes in the results of the theoretical calculation. Unfortunately, beyond a small range that can be influenced by using a controlled mismatch between the lattice parameters of the film and the seed layer or substrate, experimentally it is not easily possible to vary the lattice parameters independent of n_{eff}.

Furthermore, as Burkert *et al.* point out,[24] the degree of long-range chemical order also has significant influence on

the magnetocrystalline anisotropy. Following their estimate in experimental samples with a degree of chemical order in the range of 0.85 to 0.95 a reduction of the anisotropy compared to the theoretical values by about 10% is predicted. Together the values assumed for the c/a ratio in Ref. 24 and the imperfections of the experimental samples studied here may explain some of the quantitative discrepancy between theoretical predictions and experimental results. However, the antiparallel alignment of the Fe and Mn moments observed in XMCD measurements of samples over the entire composition range, the observation of canted magnetic and antiferromagnetic phases in an earlier neutron diffraction study,[27] and the absence of any indication for the enhancement of the magnetocrystalline anisotropy for $x \leqslant 0.25$ predicted in Ref. 24 seem to hint at a more qualitative and fundamental discrepancy between theoretical description and experimental realization.

ACKNOWLEDGMENTS

We are indebted to A. K. Kellock for PIXE and RBS analyses, and D. Pocker for x-ray photoemission measurements. We would like to thank K. R. Coffey, M. Liberati, T. Suzuki, H. Ohldag, E. F. Fullerton, S. Maat, and J. Stohr for many fruitful discussions. G. M. is grateful for funding by the Alexander von Humboldt Foundation, Bonn (Germany).

[1] A. Sakuma, J. Phys. Soc. Jpn. **63**, 3053 (1994).
[2] E. Raub and W. Mahler, Z. Metallkd. **46**, 210 (1955).
[3] M. J. Besnus and A. J. P. Meyer, Phys. Status Solidi B **58**, 533 (1973).
[4] G. E. Bacon and J. Crangle, Proc. R. Soc. London, Ser. A **272**, 387 (1963).
[5] O. A. Ivanov, L. V. Solina, V. A. Demshina, and L. M. Magat, Fiz. Met. Metalloved. **35**, 92 (1973).
[6] V. V. Maykov, A. Y. Yermakov, G. V. Ivanova, V. I. Khrabrov, and L. M. Magat, Fiz. Met. Metalloved. **67**, 79 (1989).
[7] A. Cebollada, D. Weller, J. Sticht, G. R. Harp, R. F. C. Farrow, R. F. Marks, R. Savoy, and J. C. Scott, Phys. Rev. B **50**, 3419 (1994).
[8] D. Weller and M. F. Doerner, Annu. Rev. Mater. Sci. **30**, 611 (2000).
[9] D. Vasumathi, A. L. Shapiro, B. B. Maranville, and F. Hellman, J. Magn. Magn. Mater. **223**, 221 (2001).
[10] M. Auwarter and A. Kussmann, Ann. Phys. **7**, 169 (1950).
[11] A. F. Andresen, A. Kjekshus, R. Mollerud, and W. B. Pearson, Philos. Mag. **11**, 1245 (1965).
[12] R. Y. Umetsu, M. Miyakawa, K. Fukamichi, and A. Sakuma, Phys. Rev. B **69**, 104411 (2004).
[13] E. Kren, G. Kadar, L. Pal, J. Solyom, P. Szabo, and T. Tarnoczi, Phys. Rev. **171**, 574 (1968).
[14] R. F. C. Farrow, R. F. Marks, S. Gider, A. C. Marley, S. S. P. Parkin, and D. Mauri, J. Appl. Phys. **81**, 4986 (1997).
[15] O. N. Mryasov, J. Magn. Magn. Mater. **272-276**, 800 (2004).
[16] U. Nowak, O. N. Mryasov, R. Wieser, K. Guslienko, and R. W. Chantrell, Phys. Rev. B **72**, 172410 (2005).
[17] K. R. Coffey, M. A. Parker, and J. K. Howard, IEEE Trans. Magn. **31**, 2737 (1995).
[18] J.-U. Thiele, M. E. Best, M. F. Toney, and D. Weller, IEEE Trans. Magn. **37**, 1271 (2001).
[19] T. Suzuki and K. Ouchi, IEEE Trans. Magn. **37**, 1283 (2001).
[20] T. Suzuki, Z. G. Zhang, A. K. Singh, J. H. Yin, A. Perumal, and H. Osawa, IEEE Trans. Magn. **41**, 555 (2005).
[21] C. P. Luo, S. H. Liou, L. Gao, Y. Liu, and D. J. Sellmyer, Appl. Phys. Lett. **77**, 2225 (2000).
[22] T. Shima, K. Takanashi, Y. K. Takahashi, and K. Hono, Appl. Phys. Lett. **85**, 2571 (2004).
[23] R. F. C. Farrow, D. Weller, R. F. Marks, M. F. Toney, S. Horn, G. R. Harp, and A. Cebollada, Appl. Phys. Lett. **69**, 1166 (1996).
[24] T. Burkert, O. Eriksson, S. I. Simak, A. V. Ruban, B. Sanyal, L. Nordstrom, and J. M. Wills, Phys. Rev. B **71**, 134411 (2005).
[25] T. Suzuki, H. Kanazawa, and A. Sakuma, IEEE Trans. Magn. **38**, 2794 (2002).
[26] J.-U. Thiele, K. R. Coffey, M. F. Toney, J. A. Hedstrom, and A. J. Kellock, J. Appl. Phys. **91**, 6595 (2002).
[27] A. Z. Menshikov, V. P. Antropov, G. P. Gasnikova, Y. A. Dorofeyev, and V. A. Kazantsev, J. Magn. Magn. Mater. **65**, 159 (1987).
[28] A. Cebollada, R. F. C. Farrow, and M. F. Toney, in *Magnetic Nanostructures*, edited by A. Nalwa (American Scientific, Stevenson Ranch, CA, 2002), p. 93.
[29] K. Barmak, J. Kim, L. H. Lewis, K. R. Coffey, M. F. Toney, A. J. Kellock, and J.-U. Thiele, J. Appl. Phys. **98**, 033904 (2005).
[30] H. Miyajima, K. Sato, and T. Mizoguchi, J. Appl. Phys. **47**, 4669 (1976).
[31] E. Arenholz and S. O. Prestemon, Rev. Sci. Instrum. **76**, 083908 (2005).
[32] R. F. C. Farrow, D. Weller, R. F. Marks, M. F. Toney, A. Cebollada, and G. R. Harp, J. Appl. Phys. **79**, 5967 (1996).
[33] J.-U. Thiele, L. Folks, M. F. Toney, and D. K. Weller, J. Appl. Phys. **84**, 5686 (1998).
[34] R. Nakajima, J. Stohr, and Y. U. Idzerda, Phys. Rev. B **59**, 6421 (1999).
[35] Y. Yonamoto, T. Yokoyama, K. Amemiya, D. Matsumura, and T. Ohta, Phys. Rev. B **63**, 214406 (2001).
[36] J. Stohr and R. Nakajima, IBM J. Res. Dev. **42**, 73 (1998).
[37] O. Rader, W. Gudat, D. Schmitz, C. Carbone, and W. Eberhardt, Phys. Rev. B **56**, 5053 (1997).
[38] B. Dai, J. W. Cai, W. Y. Lai, Y. K. An, Z. H. Mai, F. Shen, Y. Z. Liu, and Z. Zhang, Appl. Phys. Lett. **87**, 092506 (2005).
[39] O. N. Mryasov, Phase Transitions **78**, 197 (2005).
[40] M. Finazzi, L. Braicovich, C. Roth, F. U. Hillebrecht, H. B. Rose, and E. Kisker, Phys. Rev. B **50**, 14671 (1994).
[41] W. J. Antel, M. M. Schwickert, T. Lin, W. L. O'Brien, and G. R. Harp, Phys. Rev. B **60**, 12933 (1999).
[42] R. Y. Umetsu, K. Fukamichi, and A. Sakuma, Mater. Trans., JIM **47**, 2 (2006).
[43] P. Ravindran, A. Kjekshus, H. Fjellvaag, P. James, L. Nordstrom, B. Johansson, and O. Eriksson, Phys. Rev. B **63**, 144409 (2001).
[44] O. N. Mryasov, U. Nowak, K. Y. Guslienko, and R. W. Chantrell, Europhys. Lett. **69**, 805 (2005).
[45] P. Villars and L. D. Calvert, *Pearson's Handbook of Crystallographic Data for Intermetallic Phases* (American Society for Metals, Metals Park, OH, 1985).